An Update on Sizing and Performance Analysis of a Hybrid Turboelectric Regional Jet for the NASA ULI Program

Christopher Perullo[1], Mingxuan Shi[2], Gokcin Cinar[3], Alan Alahmad[4], Mitchell Sanders[5], Dimitri N. Mavris [6]
Aerospace Systems Design Laboratory, School of Aerospace Engineering, Georgia Institute of Technology, Atlanta, GA 30332

Mike J. Benzakein[7]
The Ohio State University, Columbus, OH 43210

Under the NASA University Leadership Initiative (ULI) program, a team of universities are collaborating on the advancement of technologies a hybrid turboelectric regional jet, with an intent to enter service in the 2030 timeframe. In the previous studies of the ULI program, the in-service benefits of the technologies under development were analyzed by integrating the technologies of interest to a 2030 regional jet with a hybrid turbo-electric distributed propulsion system. As the program has progressed, the projected performances for each technology and subsystem have been updated. This paper presents an update in the sizing and performance analysis of the regional jet with the hybrid turbo-electric distributed propulsion system, by integrating the updated values of the technologies and subsystems to the vehicle. The updates in this paper include the DC/AC conversion links, efficiency of generator and cabling losses, weight of the wires, the battery cooling through the environmental control system, motor and inverter cooling by the thermal management system, and the redundancy strategy of the propulsion system. The updates of the results from the integrated model include the overall efficiency of the propulsion system, mission fuel savings, mission energy flow distribution, and the optimal hybridization rate in climb and cruise. The overall fuel saving benefit for the target 600-nmi mission is 19.9% compared to the baseline aircraft.

I. Introduction

Under the NASA ULI program, a team of researchers from The Ohio State University (OSU), Georgia Tech (GT), University of Wisconsin-Madison (UW), University of Maryland (UMD), and North Carolina A&T (NCA&T) are collaborating to develop and demonstrate electric propulsion technologies suitable for inclusion on a 2030 commercial regional jet. A previous paper assessed each technology's benefit when evaluated in an integrated manner [1]. The updates to the program presented in this paper are incorporation of efficiency maps for the IMD unit, a study on the effect of increased electrical system mass or decreased efficiency, performance of the thermal management system for the IMD units, and an optimization on the operating point of the hybrid aircraft. The team members and their roles are summarized in Fig. 1.

---

[1] Senior Research Engineer, School of Aerospace Engineering, AIAA Member
[2] Graduate Research Assistant, School of Aerospace Engineering, AIAA Student Member
[3] Research Engineer, School of Aerospace Engineering, AIAA Member
[4] Graduate Research Assistant, School of Aerospace Engineering
[5] Graduate Research Assistant, School of Aerospace Engineering
[6] S.P. Langley Distinguished Regents Professor and Director of ASDL, Georgia Tech, AIAA Fellow
[7] Assistant Vice President for Aerospace and Aviation

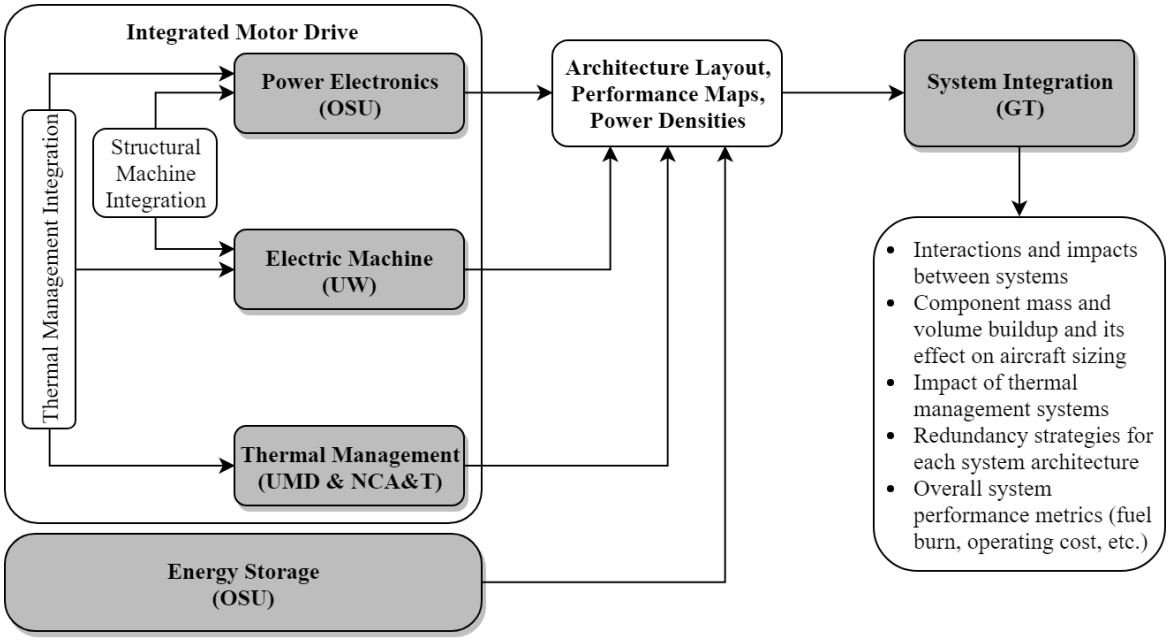

Fig. 1 Team member roles

The objectives of the ULI program consist of the development of two major turbo-hybrid-electric technology groups, an integrated motor drive unit (power electronics, electric machine, and thermal management), and a battery energy storage system. A full-scale system test is outside of the project scope; instead each subsystem will be tested at smaller demonstration sizes of 200 kW and then 1MW. Table 1 below shows the demonstration size for each subsystem and the full size on the ULI aircraft. As will be described later, a full-size regional jet with eight electrically driven fans would require 2.1 MW drives systems (each). Therefore, the 1 MW test is relevant in terms of size. All aircraft system analysis presented in this paper is with respect to the full-size aircraft.

Table 1 Subsystem Demonstration Size and Full Size on Aircraft

	Subsystem	Demonstration Size	Full Size (each fan)	Number per Aircraft
IMD	Power Electronics	1 MW	2.1 MW	8
	Electric Machine	200 kW & 1 MW	2.1 MW	8
	Thermal Management	200 kW & 1 MW	2.1 MW	8
Battery		Subscale Module	~1-2 MWh	1

1. Integrated Motor Drive Unit

The University of Wisconsin-Madison is developing and testing a 1 MW electric machine using an inner rotor surface permanent magnet configuration. The machine is designed to operate at voltages of more than 2,000 VDC while minimizing the risk of partial discharge at high altitudes. Current testing and development efforts have estimated an overall efficiency greater than 96%, with an active mass specific power greater than 23 kW/kg. University of Maryland and North Carolina A&T are designing the integrated thermal management system for the electric machine. The stator and surface mounted power electronics are oil cooled. The rotor is currently being evaluated for liquid and direct air-cooling options.

OSU is developing and testing the power electronic modules that are to be integrated with the 200 kW and 1 MW electric machines. A part of the research has focused on quantifying the effects of low pressure, high altitude environments on partial discharge and possible mitigation strategies. These findings were incorporated into the latest power module selection, which is estimated to have an overall efficiency of 98% and specific power density of 55 kW/kg. For cooling, the power modules use the same coolant loop as the electric machine stator.

The electric machine and thermal management systems will be demonstrated at both the 200 kW and 1 MW scale. The entire integrated motor drive (IMD) unit will be tested at the 1 MW scale at the NASA NEAT facility.

2. Energy Storage

The Ohio State University is designing and testing a high-performance battery module as part of the ULI aircraft's energy storage system. The team finished testing more than state-of-the-art lithium ion (NMC/graphite, with energy density ranging within 200-250 Wh/kg) cell samples. They are currently in the process of obtaining next-generation cells Li-Sulfur cells with energy density above 300 Wh/kg. The results obtained from many of these experimental tests were utilized to create models to perform pack design and simulation studies, predicting voltage, current, heat generation, cell-to-cell SoC and temperatures given a desired power profile and other operating condition, and are used by the GT team in the aircraft sizing and assessment process.

II. Architecture of the Overall Systems

A. Baseline and Next-Gen Architecture and Assumptions

The ULI aircraft is a regional jet capable of carrying 86 passengers 1,980 nautical miles. Two reference aircraft were also modeled: the Baseline aircraft and the Next-Gen aircraft. The Baseline aircraft architecture has two conventional turbofans mounted under the wings and is intended to replicate the performance of a CRJ900 sized aircraft. In order to isolate the impact of turbo-hybrid electric propulsion, the Baseline aircraft was morphed into a Next-Gen aircraft by assuming +10-year technologies applied to the aircraft weights, aerodynamics, and turbomachinery efficiency and cooling. The values used were consistent with prior studies [2].

B. ULI Aircraft Architecture

The ULI aircraft architecture is a hybrid turboelectric distributed propulsion (HTeDP) system with two wing tip mounted turbo generators providing electrical power to eight IMD driven fans. Fig. 2 provides an overview of the ULI aircraft architecture. The aircraft assumes the same technology improvements for the structural weight, drag, and engine components as the Next-Gen aircraft previously described. At shorter ranges, the aircraft does not need to carry as much fuel to complete the trip. As a result, it is then able to carry additional batteries, with the intention to decrease the block fuel consumption for these missions.

There are two main types of thermal management systems (TMS) for the electric propulsion system. One of them is for the IMDs on each side of the wing, and the other is for the energy storage system (battery). Each IMD is cooled using an air-cooled oil cooler (ACOC) with the cooling air being supplied by fan duct. The battery packs stored in the floor of the aircraft are cooled using air from the existing environmental control system (ECS). Details regarding TMS modeling and impacts are found in Sec. II-E.

C. Propulsion System Modeling

The HTeDP architecture was modeled using NPSS and Georgia Tech's GT-HEAT model. GT-HEAT is designed specifically for modeling and evaluation of unconventional, highly integrated aircraft concepts [3]. The propulsion architecture is shown below in Fig. 3. The turbo-generators were modeled as a two-spool architecture with an additional power-generating turbine on a free shaft. The orange components in Fig. 3 represent the electrical system unique to the ULI aircraft. OSU provided the battery pack model created using test data from a number of commercial and prototype cells. The motor and inverter efficiencies have been updated to use performance maps developed by UMD and OSU, this is explained in more detail below. Generator design is out of the scope of the ULI project, but it is assumed that many of the technologies developed for the IMD would transfer over in terms of benefit and efficiency levels.

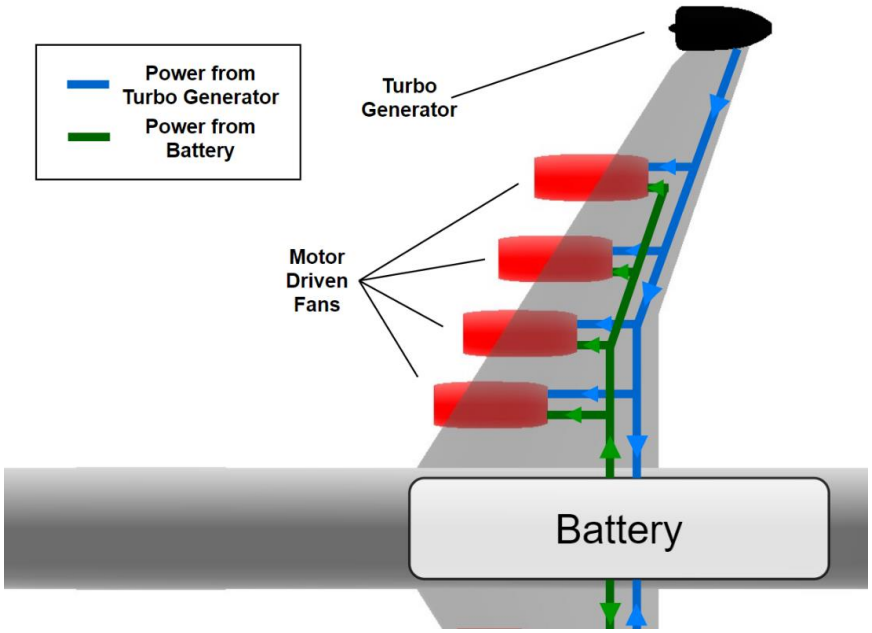

Fig. 2 Illustration of ULI aircraft propulsion system architecture

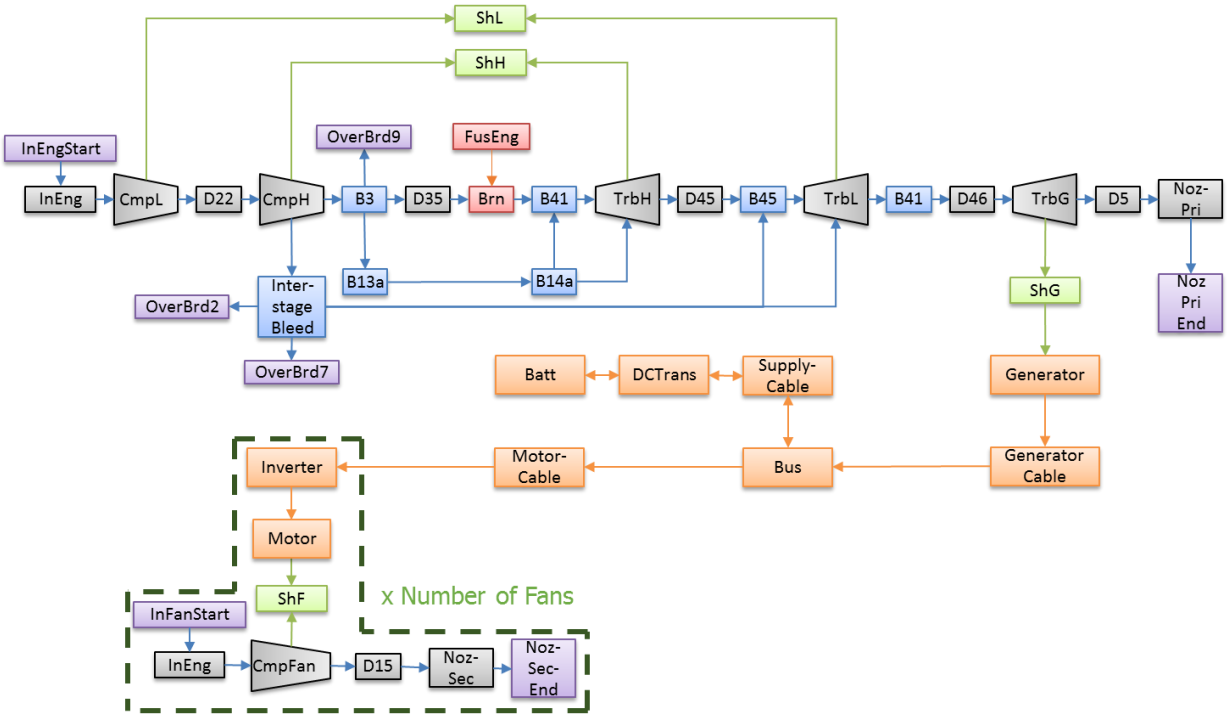

Fig. 3 HTeDP architecture as modeled in NPSS

Previously, GT-HEAT had been using a first order analytical model for predicting motor efficiency throughout the mission. The new motor efficiency model uses a scaled efficiency map provided by UMD that is a function of the motor shaft speed and torque. The efficiency map is currently model based but will be updated to reflect experimental data once it becomes available. Fig. 4 shows the scaled efficiency map with an overlay of the off-design hybrid

mission. The key points throughout the mission are labeled on this figure. Note that a gearbox will be required, and fan speed is shown in the figure below, not motor shaft speed which is higher.

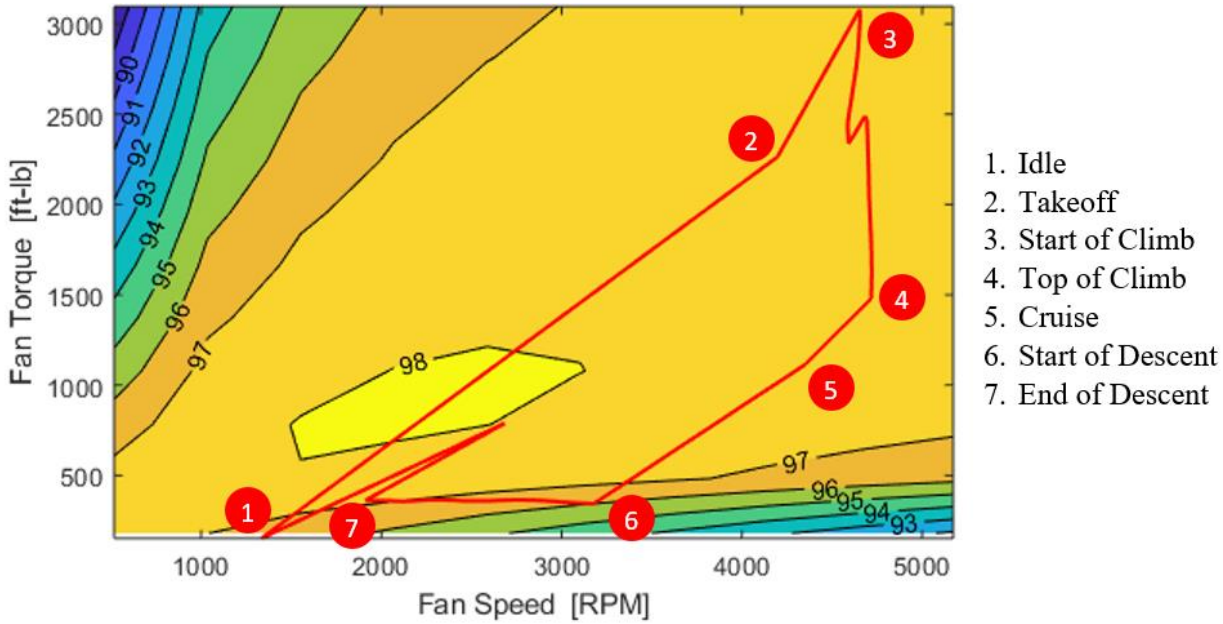

Fig. 4 Scaled motor efficiency map overlaid with typical off-design hybrid mission (%)

The new inverter efficiency model is based on an efficiency curve provided by OSU CHPPE that is a function of the output power. This efficiency map is also model based but will be updated to reflect experimental data once it becomes available. Fig. 5 below shows the scaled efficiency map with an overlay of points from the off-design hybrid mission; the key points throughout the mission are also labeled.

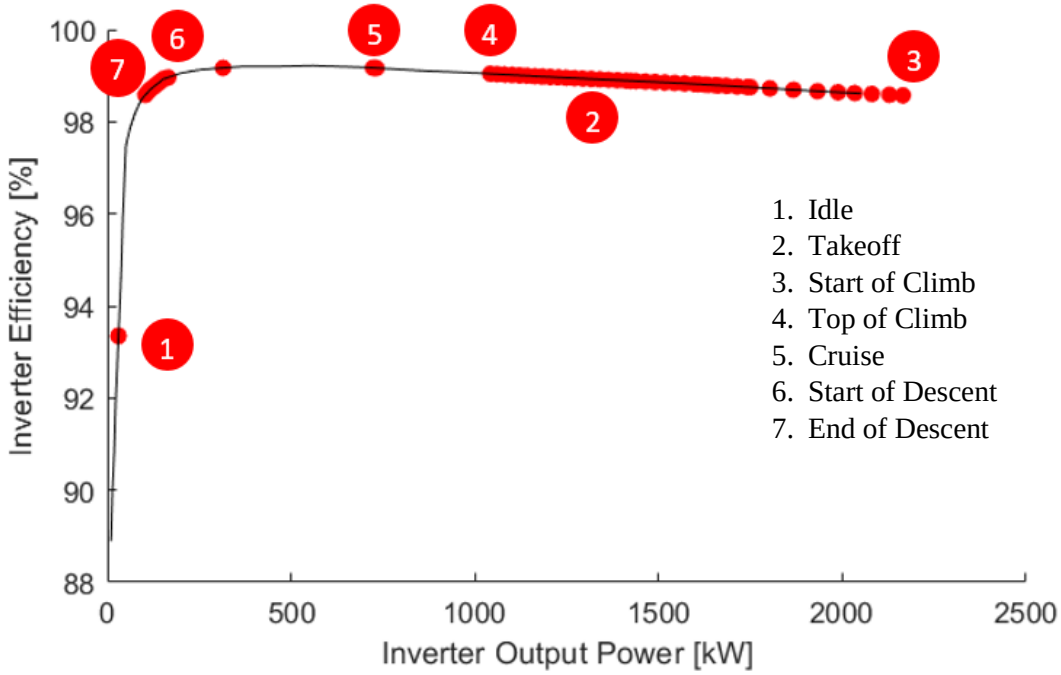

Fig. 5 Scaled inverter efficiency map overlaid with off-design hybrid mission

The GT-HEAT model includes fixed efficiency values for the DC/AC conversion links, generator, and cabling losses since their design is not in the scope of this project. Each electrical component's mass is also determined using

a fixed specific power value and the design power it is sized at. The estimates for these values represent the current state-of-the-art for these components and is shown below in Table 2. The overall specific power of the entire system is estimated at 5.46 kW/kg.

Table 2 Electrical System Component Efficiencies and Specific Power

Component	Efficiency
Generator	97%
Rectifier	99%
Bus	99%
Inverter	From Map
Motor	From Map
Cabling	100%

In the case that the fixed efficiency values are lower than estimated or component mass is higher than estimated, a trade study was run to determine their effect on overall aircraft performance, specifically block fuel burn. Instead of doing a parametric study on each electrical component, the overall efficiency and specific power values were decreased by a certain percentage. Since this study requires the use of a sized aircraft, the results are shown below in Sec. III-C.

D. Power Generation and Distribution System

A bus multi-feeder architecture of the power generation and distribution system (PGDS) is selected for the current ULI aircraft because it has the lowest weight penalty, of which the architecture is presented in Fig. 6.

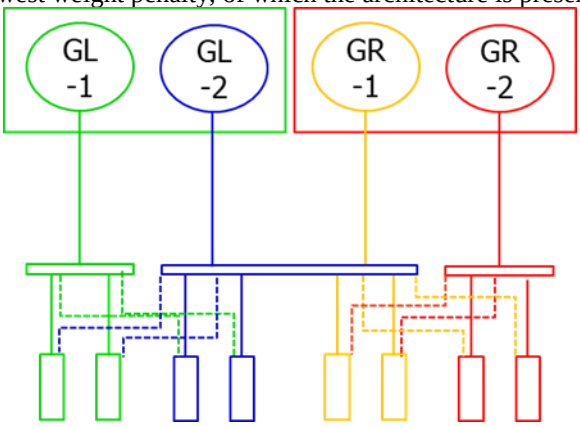

Fig. 6 Architecture of the bus multi-feeder PGDS

E. Thermal Management System Modeling

Two aircraft level TMS, namely, the battery TMS and the IMD unit TMS, were modeled for the ULI aircraft. The overall TMS architecture is shown in Fig. 7. The battery pack is air cooled using the existing environmental cooling system (ECS) on the aircraft. The battery pack is allowed to heat up over the mission with an imposed temperature limit of 45°C to preserve battery life. An ECS similar to the architecture of a CRJ700/900 ECS was modeled in NPSS, and any excess cooling capacity from the ECS is used to cool the battery if required. Details on the ECS can be found in the previous version of this paper [1]. The modeling approach of the ECS can be found in previous work [4]. The ECS architecture is illustrated in Fig. 8.

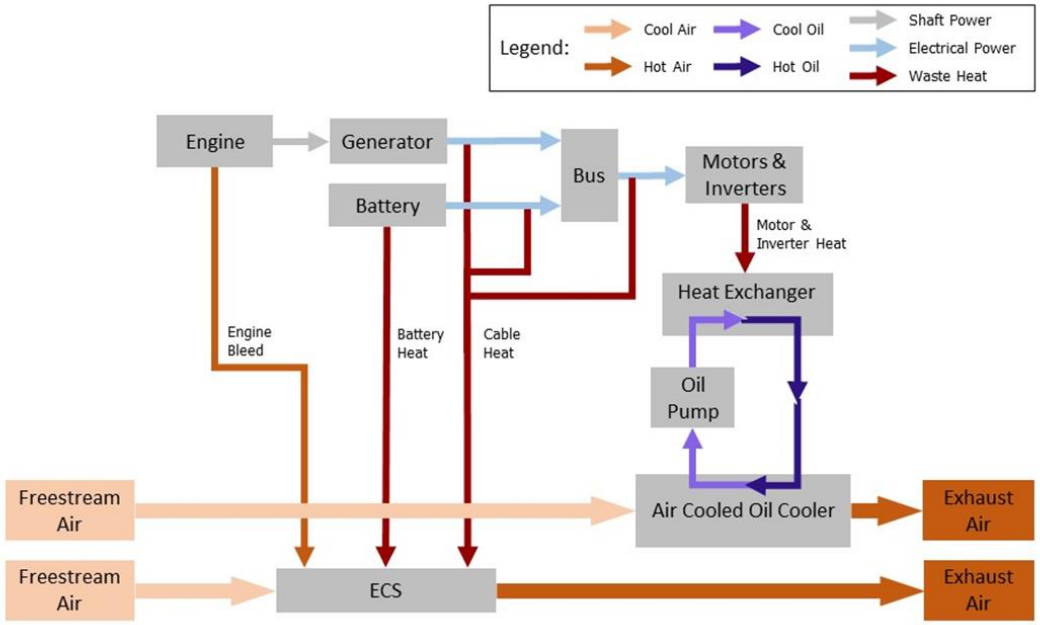

Fig. 7 Architecture of the overall TMS

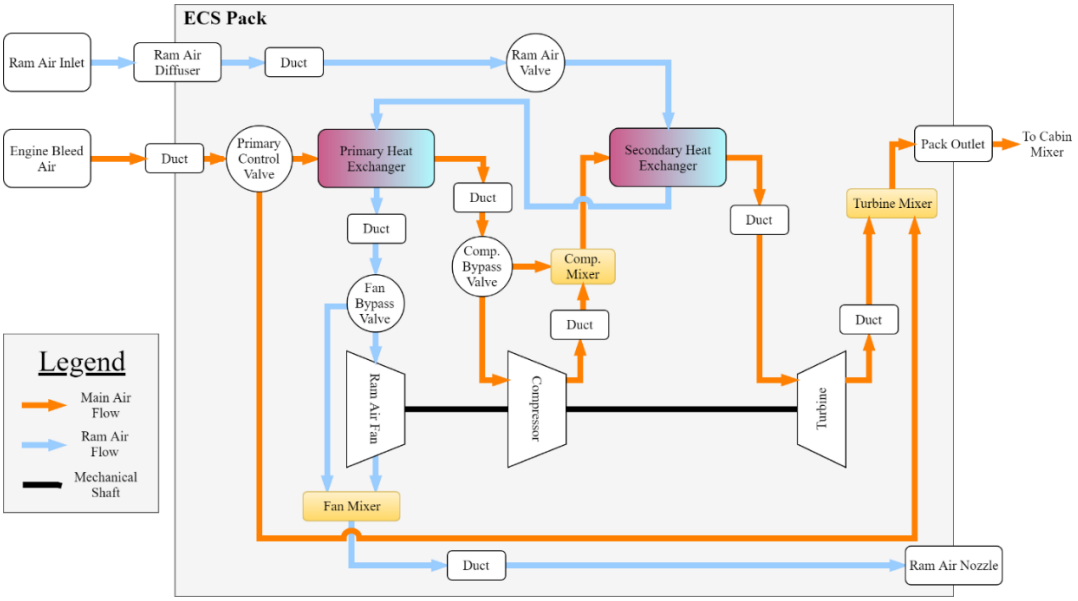

Fig. 8 Environmental control system architecture

Each IMD unit is cooled using a dedicated air-cooled oil cooler (ACOC) loop with fan duct bleed air as the cooling flow. The ACOC heat exchanger is modeled in NPSS using the ε-NTU method [5]. The ACOC heat exchanger is assumed to be a one pass tube-fin type heat exchanger, with flat tubes containing Polyalphaolefin (PAO) fluid that is cooled by fan duct air that passes through the fins, of which the detailed implementation can be also found in the authors previous work [4]. PAO fluid was chosen instead of jet engine oil, mainly because of the lower operating temperatures of electric motors and inverters (jet engine oil would be too viscous at lower temperatures). The heat exchanger model was integrated into the system level GT-HEAT model to ensure that the fans are properly sized to account for the pressure drop and temperature rise of air passing through the heat exchanger. The sizing condition for the IMD TMSs is at takeoff (0 ft, Mach 0.3). Heat loads and target temperature limits for each electrical component were provided by the partner universities and used to size the ACOC. The corresponding TMS architecture is shown

in Fig. 9. The heat generation and heat removal performances for a typical mission (600 nmi and 38 passengers) for a single IMD (there are 8 IMD in total for the whole aircraft) is shown in Fig. 10(a), and the corresponding power difference between the heat removal and the generation is presented in Fig. 10(b). It can be discovered from these figures that the generated heat cannot be fully removed during early mission segments where the thermal load of the IMD is at the peak. The total heat that cannot be removed for this selected mission for the whole vehicle is 40,736 kJ.

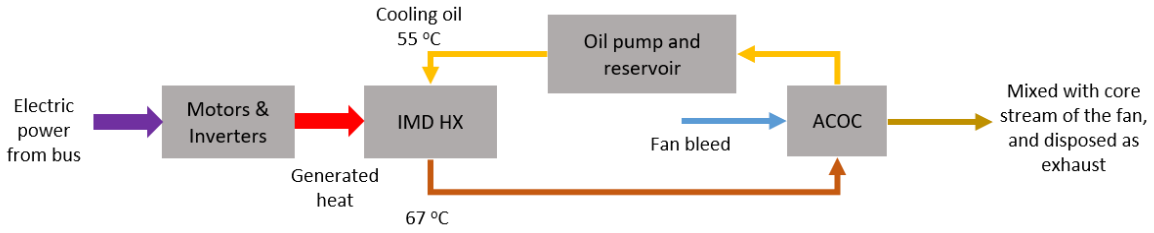

Fig. 9 Thermal management system architecture

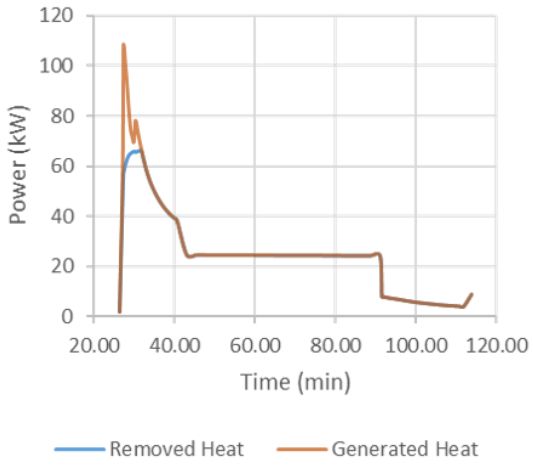

(a) Heat removal and generation for a single IMD through the selected mission

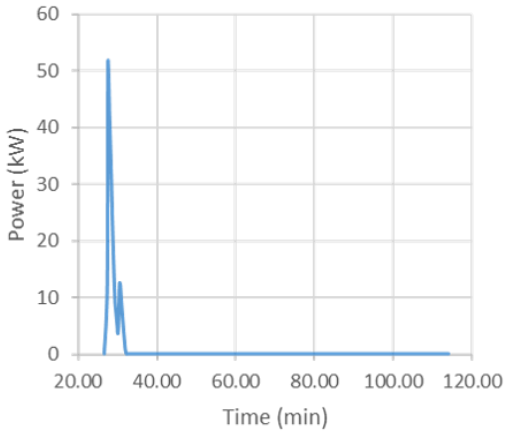

(b) Power difference between heat removal and generation for a single IMD

Fig. 10 Performance of heat removal and generation for the selected mission (600 nmi and 38 passengers)

Therefore, a solution by implementing additional PAO to handle such peak thermal load is proposed. The architecture of the peak thermal load solution is presented in Fig. 11. There is a cold oil reservoir (55 °C) and a hot oil reservoir (67 °C). The cold reservoir supplies the cooling oil to the IMD heat exchanger, which the oil that can be cooled to the target temperature (55 °C) is also looped in. For the portion of the oil that cannot be cooled, it is directly transmitted to the hot oil reservoir. Such architecture can maximize the heat storage capacity of the PAO because it maximizes the oil temperature in the hot oil reservoir. More details regarding the TMS as well as the heat absorption solution can be found in the accompanying paper [6], which discusses the details of the design and analysis of the TMS. The performances of the IMD heat generation and removal for a single IMD with the proposed heat absorption solution using additional PAO for a single IMD is plotted in Fig. 12. The required additional PAO flow for a single IMD through the mission is shown in Fig. 13. Comparing Fig. 10(a) and Fig. 12, it can be seen that the heat that cannot be handled during early mission segments can be removed by the proposed heat absorption solution. However, implementation of such a solution adds penalty weight to the aircraft due to the additional PAO. The additional weight for the thermal mass and systems is estimated to be around 3,600 lbm, where the computation approach is also shown in the accompanying paper [6]. It should be noted that the current results do not include the impacts of the heat absorption architecture in IMD TMS which utilizes additional PAO because the ULI team is still working on the development of the IMD TMS to identify the optimal solution to handle the heating problem during early mission segments.

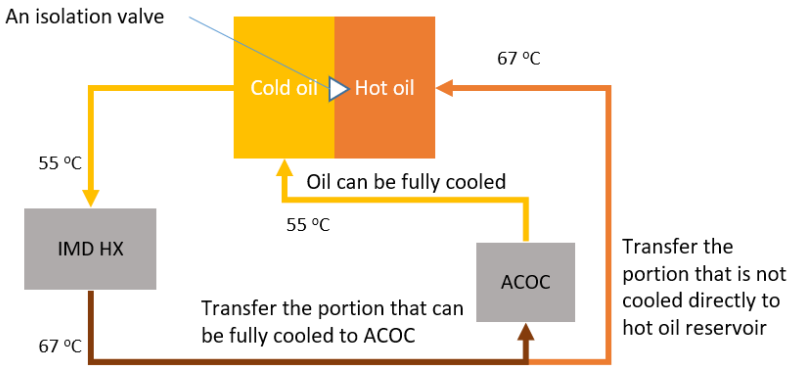

Fig. 11 Additional PAO to absorb heat during early mission segments

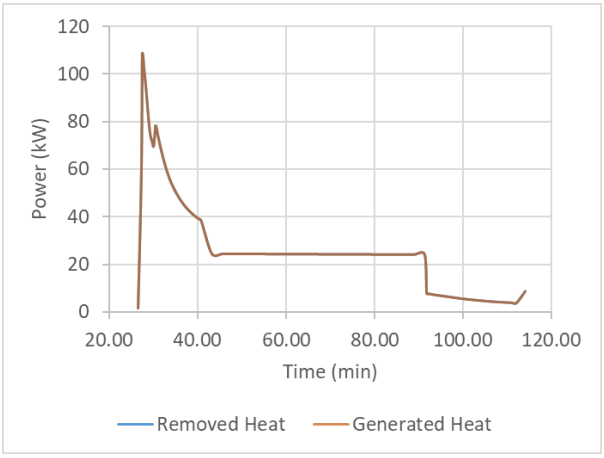

Fig. 12 Heat removal and generation for a single IMD with heat absorption solution using additional PAO

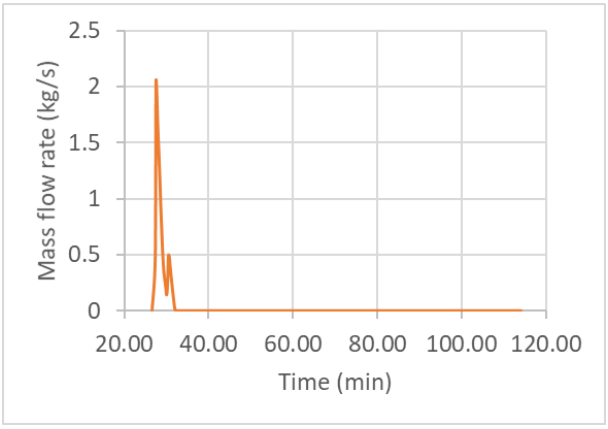

Fig. 13 Additional PAO mass flow rate for a single IMD

The IMD TMS also influences the mission-level performance in the following ways: an additional pressure drop occurs to the cooling fan bleed as it passes through the ACOC heat exchanger which affects the thrust produced by the fan; additional weights are also added due to the installation of the heat exchangers, ducts and the coolant reservoir, as well as the weight of the PAO, which all contribute to additional aircraft weight. The pressure drop in the cooling fan bleed, the weight of PAO in the ACOC heat exchanger, the weight of the heat exchanger are calculated using the heat exchanger model which is created based on Kays and London's book [5]. The PAO volume in the IMD HX is given by the team from University of Maryland, which is 6.5 L for a 1-MW IMD. Assuming the same volumetric density, this number is scaled to a 2.1-MW IMD by simply multiplying 2.1, where the 2.1-MW IMD is supposed to

be applied for a full scale ULI aircraft. All these influences of the IMD TMS on the mission-level performance can be seen from the resulted block fuel burn, which will be discussed in Sec. III-A and Sec. III-B.

F. Updates in Engine Sizing Problem Setup

The engine sizing setup and corresponding results at top-of-climb (35k ft, Mach 0.8) are shown in Table 3. The setup and results for Baseline, Next-Gen, ULI Aircraft sized in 2019 (ULI 2019) configurations were accomplished in the work published last year [1]. The updates from the last paper until now are summarized under ULI 2020. The changes are resulted from the updated efficiency maps of inverter and motor. It should be noted that these specifications do not include battery system weight as the aircraft is sized to operate without the benefit of installed batteries.

Table 3 Comparison of Propulsion System Metrics at Top of Climb (Per Turbofan / Per Wing)

Metric	Units	Baseline	Next-Gen	ULI 2019	ULI 2020
Thrust per turbofan/wing	lbf	3,699	3,181	3,293	3,299
Overall Pressure Ratio (OPR)	-	34.6	53.9	59.3	58.54
Fan Pressure Ratio (FPR)	-	1.66	1.57	1.34	1.325
Bypass Ratio (BPR)	-	4.8	5.9	19.5	19.9
Specific Fuel Consumption (SFC)	lbm/lbf/hr	0.701	0.622	0.522	0.516
Turbine Inlet Temperature (T41)	°R	2,890	2,858	3,415	3,333
Generator Power	hp	-	-	5,828	5,859
Power per IMD	hp	-	-	1,358	1,371
Electric Propulsion System Weight	lbm	-	-	6,770	7,274
Engine Weight	lbm	8,800	6,300	5,990	5,450
Total Propulsion System Weight	lbm	8,800	6,300	12,760	12,724

III. Updated Results

A. Design Mission Impacts

The performance metrics of the vehicle are illustrated in Table 4, where the results for Baseline, Next-Gen, and ULI 2019 have been presented in the last paper [1], while the metrics under ULI 2020 are the updates from last year. The results for the Baseline and Next-Gen vehicles were obtained by optimization during the work in the last year, and the updates in ULI program do not influence them. Thus, the metrics for these two configurations do not change. The changes between ULI 2019 and ULI 2020 are caused by updates of the efficiency maps of the inverter and the motor, as well as the added penalty weight of the IMD TMS. Such influences will be considered in the future work once the final architecture is selected.

Table 4 Comparison of Performance Metrics for Design Mission

Aircraft Metric	Units	Baseline	Next-Gen	ULI 2019	ULI 2020
Design Mission Range	nmi	1,980	1,980	1,980	1,980
Design Payload	lbm	18,060	18,060	18,060	18,060
Operating Empty Weight	lbm	47,250	40,770	46,705	47,294
Takeoff Gross Weight	lbm	85,000	73,160	75,094	75,734
Block Fuel @ Design Mission	lbm	15,578	12,051	10,673	10,661
Mission Fuel @ Design Mission	lbm	19,690	14,329	13,286	13,288

The breakdown of the block fuel burn savings obtained in last year is shown in Fig. 14, and the updated breakdown of the block fuel burn savings in this year is shown in Fig. 15. From these two figures, it is discovered that the benefits achieved by HTeDP in ULI 2020 is improved from the results obtained in ULI 2019. This is because the motor and

inverter efficiencies were demonstrated in 2020 to be higher than the values used in 2019. However, due to the penalties caused by IMD TMS, which is a 0.8% increase of the mission block fuel burn, the total block fuel burn savings is almost the same to values from last year's analysis. It also should be noted that the hybridization is not considered for the design range mission since the aircraft is sized to operate without batteries if required or optimal for cost or CO_2 reasons.

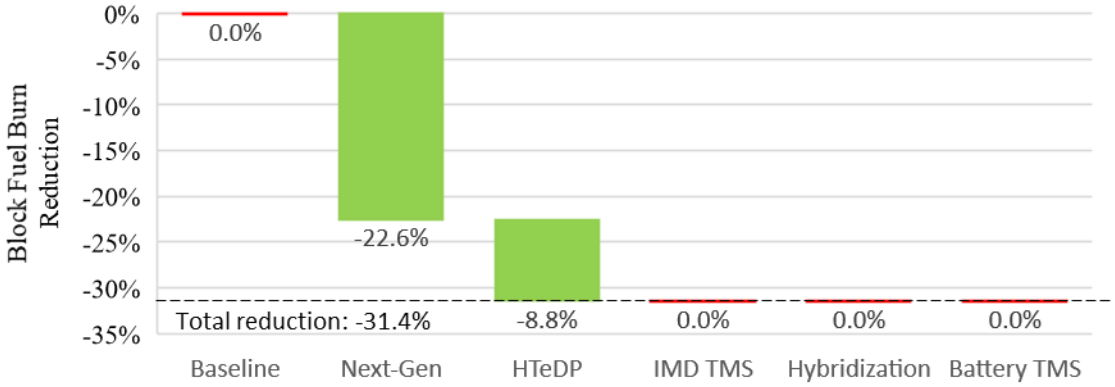

Fig. 14 Block fuel burn savings for max payload/design range mission for ULI 2019

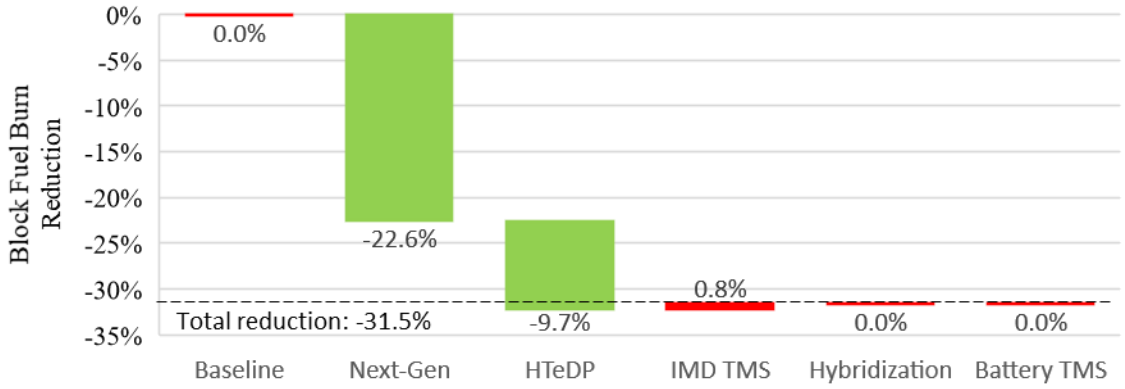

Fig. 15 Block fuel burn savings for design range mission for ULI 2020

B. Impact of Hybridization at Shorter Ranges

The ULI aircraft is designed to accommodate reconfigurable battery modules in the floor of the aircraft. For shorter-range flights where the aircraft is not typically at its MTOW, these battery modules will be used to further improve the block fuel burn savings. These batteries would not be swapped between flights, but rather the concept of operations is that each aircraft would be configured with a certain number of modules optimized for its typical daily flight schedule, similar to how conventional aircraft have add auxiliary cargo-hold fuel tanks for longer range flights.

A trade study was performed on the ULI aircraft to determine the benefit of using battery power on a 600 nmi. flight with a typical payload of the average flight for a regional jet [7]. The study was performed using a conservative energy density estimate of ~200Wh/kg at the pack level (depends on usage profile of the battery). The fraction of power coming from the battery when measured at the bus was varied between 0-30% for climb and 0-50% for cruise. These fractions mean the percentage of energy is supplied by the battery for climb or cruise. Fig. 16 shows a contour plot of fuel burn savings compared to a non-hybrid mission (still HTeDP configuration). Two constraints were also considered. First, the takeoff weight of the aircraft including batteries must not exceed the maximum takeoff weight of the aircraft. This MTOW constraint is denoted by the red constraint line. As power usage from the battery increases, more power is needed from the battery, which may lead to a larger battery weight, making the MTOW violate the constraint. The second constraint was that the ECS must be able to keep the battery below the 45°C temperature limit through the whole mission. The two yellow lines in this figure denote the maximum temperature constraint. In ULI 2020, The operation schedule of the battery TMS (ECS), was optimized in terms of different batter usages to minimize the battery cooling penalties which include engine bleed extraction and the intake of additional ram air, while the

battery cooling penalties were fixed for any battery power usages in year 2019. The star in the figure (climb battery power fraction = 0.17, cruise battery power fraction = 0.235) denotes the optimal battery usage fraction among climb and cruise that minimizes the block fuel burn. As a result of considering the battery TMS impacts in terms of different battery usages, the resulted optimal power fraction is far away from the battery temperature limit, minimizing the battery cooling penalties.

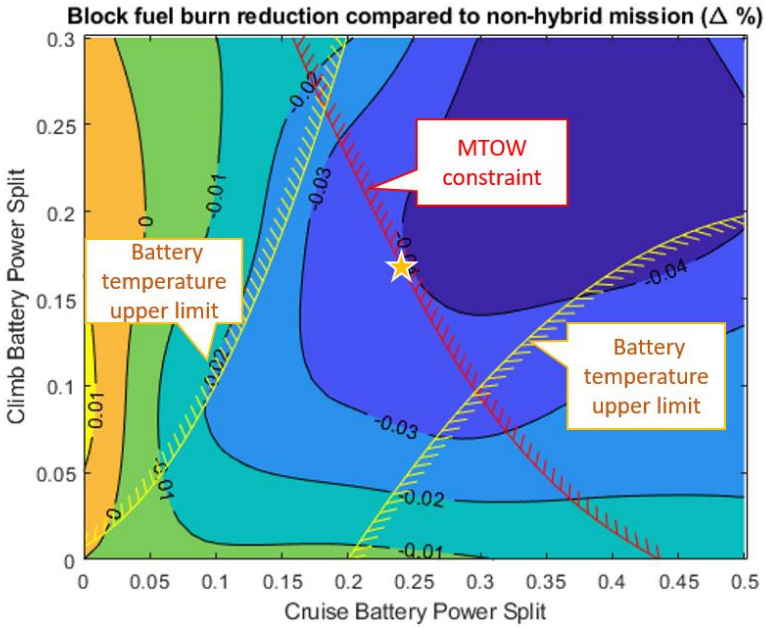

Fig. 16 Block fuel burn reduction compared to non-hybrid mission with different battery usages (Δ%)

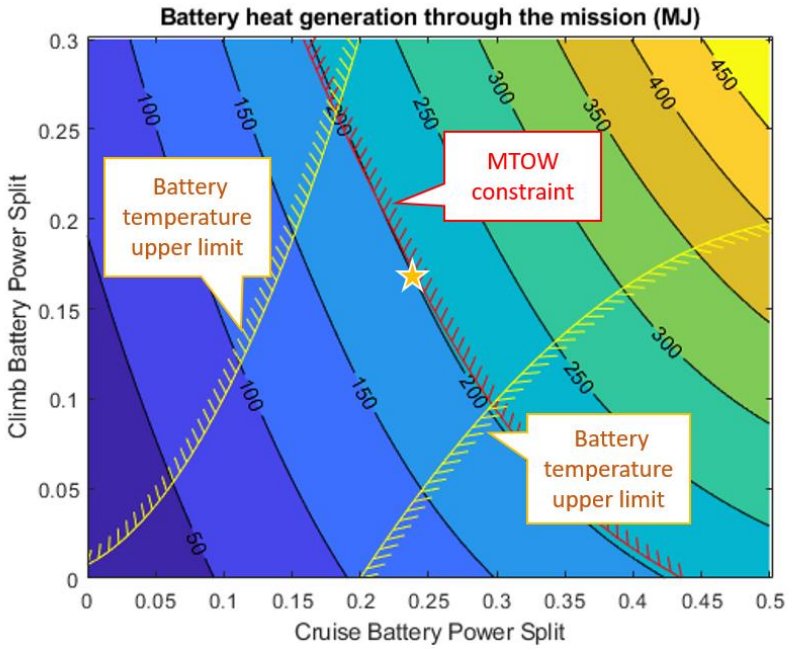

Fig. 17 Battery heat generation through the mission for different battery usages (MJ)

With the all the updates as mentioned above and the obtained optimal battery usage fraction, the updated block fuel burn saving can be obtained. The breakdown of the block fuel burn saving for the selected 600-nmi off-design mission for ULI 2019 is presented in Fig. 18, and the updated results for the same off-design mission is illustrated in Fig. 19.

The baseline and the Next-Gen performances do not change as they are not influenced by the updates in ULI 2020. The HTeDP fuel burn reduction is improved from -7.0% to -8.7% due to updates in engine component modeling. However, an additional 1.0% block fuel burn penalty is added by including the IMD TMS.

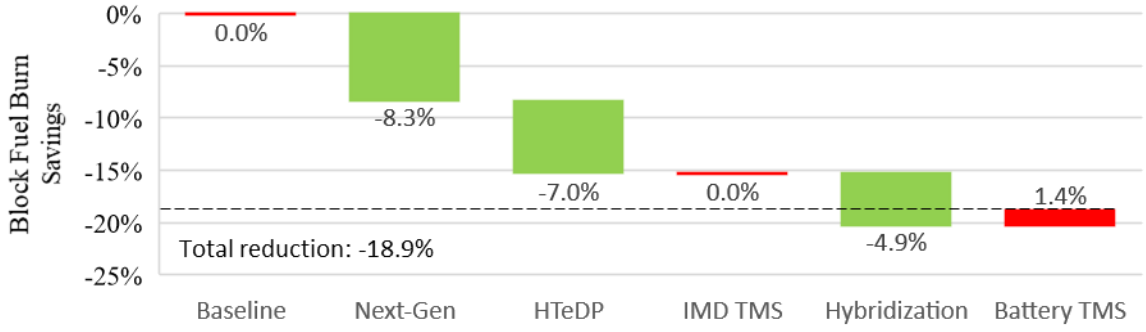

Fig. 18 Block fuel burn savings for typical payload /600-nmi off-mission for ULI 2019

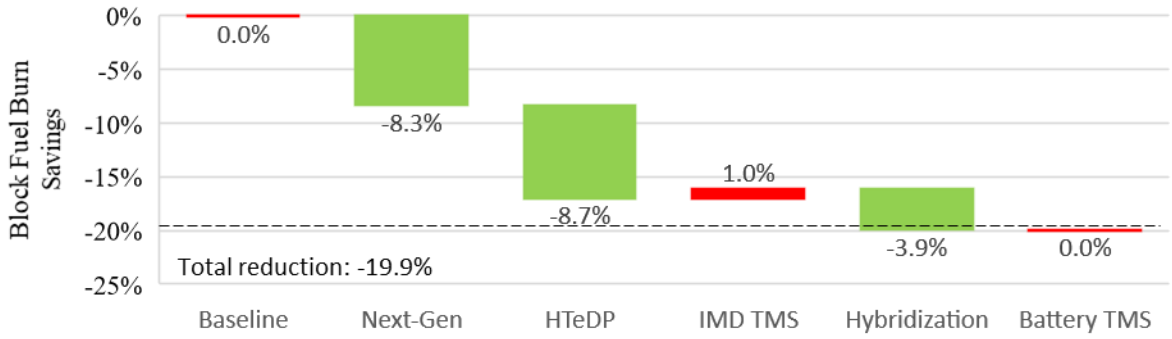

Fig. 19 Block fuel burn savings for typical payload /600-nmi off-mission for ULI 2020

C. Electrical System Weight and Efficiency Study

A sensitivity study was performed to determine the impact on aircraft performance in the case that the actual component efficiencies or specific power is lower than the estimates. This could account for any inefficiencies or additional weight from components that were not included in the model. The overall system efficiency was decreased up to -10% and specific power was decreased up to -50%, representing a doubling of the electrical system weight. A sweep of these two variables was evaluated in GT-HEAT to see their impact on mission fuel burn for both the design and off-design mission. Fig. 20 below shows the fuel burn delta of the ULI aircraft from the Next-Gen aircraft for the design mission. The upper right-most portion of the plot represents the nominal point for the ULI aircraft. Moving to the left of that represents a decrease in specific power and any point below represents a decrease in efficiency. The bolded block line represents the point where there is no fuel burn change from moving from the Next-Gen aircraft to the HTeDP system on the ULI aircraft. Fig. 21 shows the fuel burn delta of the ULI aircraft from the Next-Gen aircraft for the off-design, hybrid mission.

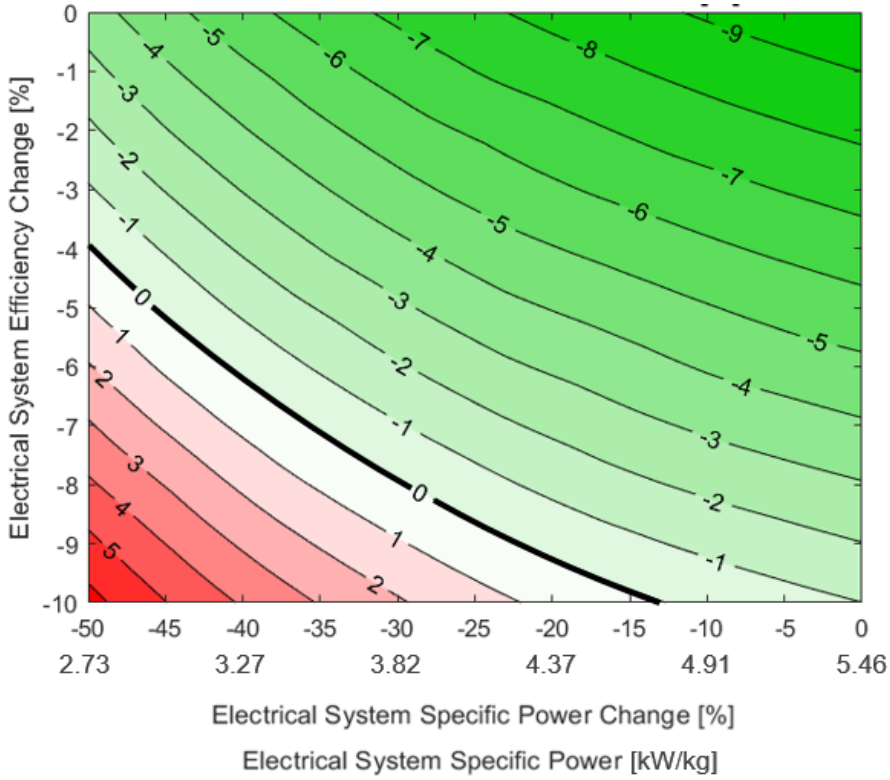

Fig. 20 Block fuel burn savings from Next-Gen aircraft for design mission (%)

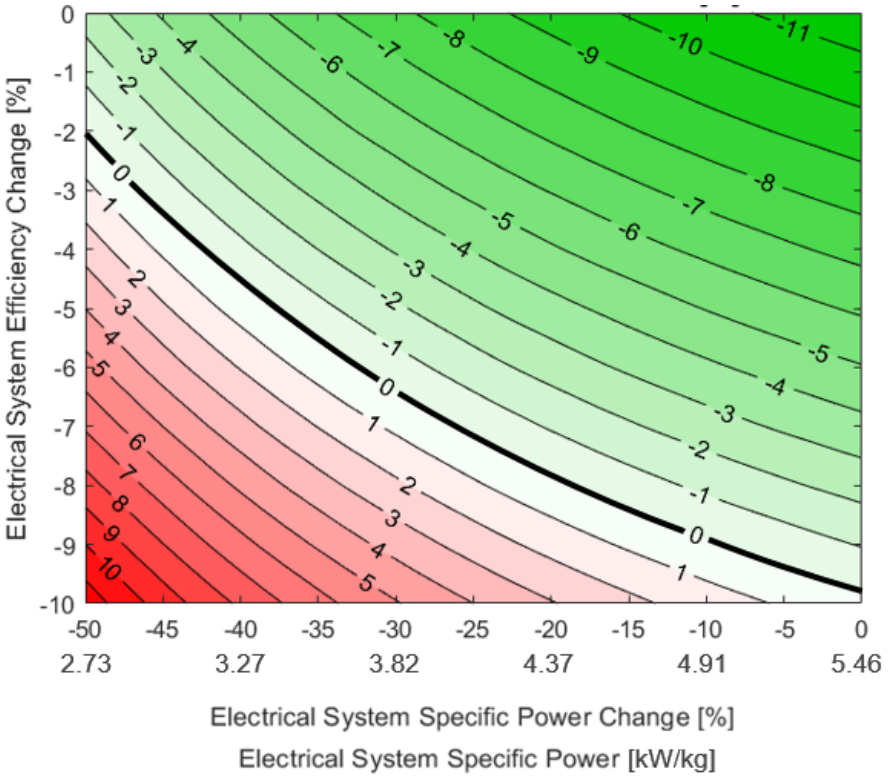

Fig. 21 Block fuel burn savings from Next-Gen aircraft for off-design hybrid mission (%)

IV. Conclusions and Future Work

This paper summarizes the updates from the work done in 2019 on projected performances of technologies and subsystems of an analysis of a 2030 hybrid turboelectric regional jet under the ULI program. The major updates on the propulsion system were that the efficiencies of the motors and inverters are calculated from the efficiency maps developed from ULI teams from multiple institutes instead of the fixed values as used in the last year. Such updates on the propulsion system improved the fuel economy performance of the HTeDP configuration compared to the results from the last year. Regarding the power generation and distribution system, two new strategies were proposed, and the corresponding weight penalties were also assessed for the all six strategies. In terms of the system integration, the IMD was integrated with its TMS to analyze the cooling capability of the IMD TMS and the corresponding system-level and mission-level impacts. It was discovered that the heat generated by the IMD cannot be fully removed by the TMS during early mission segments where the thermal load is the largest. Therefore, a heat absorption solution for such mission segments may be required. In addition, the IMD TMS poses an additional pressure drop to the fan flow as well as adding penalty weight to the whole system due to installation of ACOC heat exchangers and PAO coolant. This paper has shown that such impacts increased the empty weight of the vehicle and leaded to an increase in the block fuel burn in both design and off-design missions. The battery cooling is still conducted by using additional ECS cooling power, and the corresponding cooling architecture is the same as previous work. However, the dependencies between the penalties due to battery cooling and battery power usage were considered in this year while such dependencies were not included in 2019. The resulted optimal battery usage profile in this year presented an overall fuel burn benefit over the one obtained in the last year when consider battery cooling, indicating neglecting these dependencies may lead to a suboptimal battery usage decision. A breakdown of the block fuel burn savings considering all the updates this year is also presented in contrast to the results from the last year, illustrating the mission-level changes as the ULI program progresses.

The Georgia Tech ULI team will continue updating the assessment of the aircraft as refined technology development information becomes available. Another research avenue is to investigate further in searching for the optimal heat removal solution during early mission segments.

Appendix A: Aircraft Specification Sheet

Propulsion Architectural Schematic

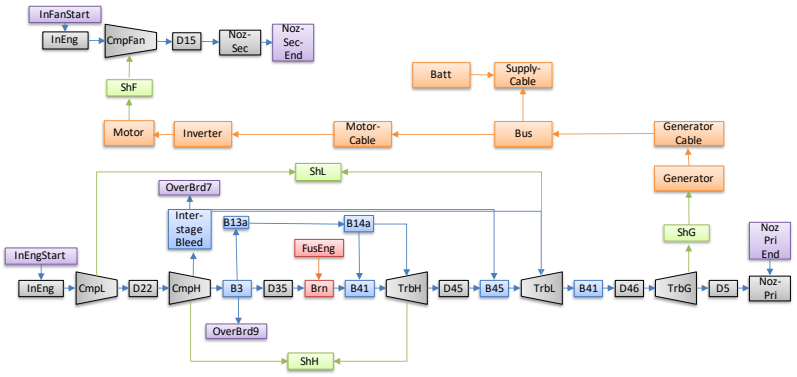

ULI Aircraft Concept

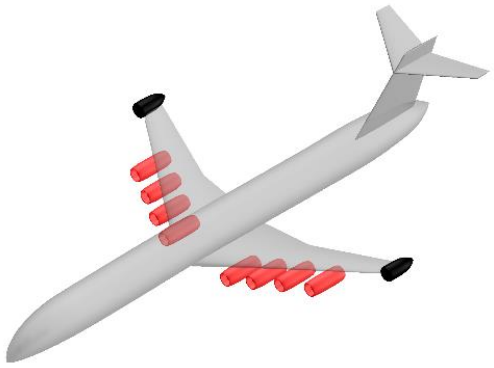

Propulsion Architecture Metrics (35k ft / Mach 0.8 / Top of Climb Power)	**ULI SI Units**	**Baseline SI Units**	**ULI Imperial Units**	**Baseline Imperial Units**	**Delta**
Specific Thrust (N/kg or lbf/lbm)	4.31	8.13	0.44	0.83	-38%
Thrust Specific Fuel Consumption (lbm/lbf-hr)			0.50	0.69	-25%
Global Chain Efficiency (-)	35.0%	28.0%			

Typical Mission Profile		**Power Management, Allocation and Control Strategy**
Stage Length (nm)	600	
Taxi-out (min.)	26	Idle power
Take-off (min.)	0.75	Max takeoff power
Climb (min.)	13	Max climb (full fan flow, keep gas generator thrust to minimum)
Cruise (min.)	52	Thrust = Drag
Descent (min.)	21	Idle power
Approach (min.)	2	Idle power
Taxi-in (min.)	5	Idle power
Diversion (nm)	100	Same as regular mission

Aircraft Design Weights	**ULI SI Units**	**Baseline SI Units**	**ULI Imperial Units**	**Baseline Imperial Units**	**Delta**
Maximum Take-Off Weight (kg or lbm)	33,352	38,555	75,734	85,000	-11%
Operat. Weight Empty or Basic Oper. Weight (kg or lbm)	21,452	21,432	47,296	47,250	0.1%
Maximum Payload Weight (kg or lbm)	10,594	10,594	23,350	23,350	-
Max Fuel Weight (kg or lbm)	7,072	8,934	15,493	19,690	-21%
Aircraft Sizing Parameters and Metrics					
Reference Wing Area (m^2 or sq.ft)	69.9	69.6	753	749	0.5%
Reference Wing Aspect Ratio (-)			8.29		-
Conditions Describing Total Maximum Thrust or Power	Rolling Takeoff (Mach 0.25 / ISA + 18 F (10 C))				
Total Maximum Thrust (kN or lbf)	102.5	115.0	23,048	25,846	-11%
Total Maximum Power (kW or hp)	19,617	-	26,307	-	-
Max. Non-propulsive Power / Total Max. Power (-)	~2%	~2%			
Peak Battery Thermal Load (kW or hp)	1,486	-	1,993	-	
Peak IMD Thermal Load (kW or hp)	880		1,180		

Operational Performance	**ULI SI Units**	**Baseline SI Units**	**ULI Imperial Units**	**Baseline Imperial Units**	**Delta**
Payload (kg or lbm) Specified ISA Deviation (°C) Specified Airport Elevation, AGL (ft)	8,194 +0 0	8,194 +0 0	18,060 +0 0	18,060 +0 0	-
Maximum Operating Altitude (ft)			41,000	41,000	-
Climb Speed Schedule (KCAS/Mach)			250 [0.8]	250 [0.8]	
Maximum Rate-of-Climb, MTOW b.r., ISA, SL (fpm)			2,560	2,000 – 3,000* Depends on battery usage	*Depends on hybrid sched.*
Time-to-Climb to Initial Cruise Altitude (min.)	31.0	40.0			10 min
Initial or Fixed Cruise Altitude, MTOW b.r., ISA (ft)			30,000	35,000	
Typical Cruise Speed, Mach [KTAS]			0.8 [461]	0.8 [461]	-
Typical Cruise Lift-to-Drag (-)	~16.2	~16.0			1%

Max. PAX/Payload Design Range	Range (nmi or km) and [PAX]	3,667 [78]		1980 [78]		
	Payload (kg or lbm)	8,194	8,194	18,060	18,060	-
	Block Fuel (kg or lbm)	4,836	7,068	10,661	15,578	-32%
	CO_2-Emissions (kg or lbm)	18,123	26,716	39,955	58,883	-32%
	Block Fuel per PAX (kg/PAX or lbm/PAX)	62	90	137	199	-32%
	CO_2-Emissions per PAX (kg/PAX or lbm/PAX)	232	343	512	755	-32%
	Block Energy (MWh or MBTU)	55.70	84.69	179.59	289	-32%
	Block Energy per PAX (MWh/PAX or MBTU/PAX)	0.71	1.09	2.43	3.71	
	Miss. Energy Index (Wh/kg.km or BTU/lbm.nm)	1.93	2.82	5.53	8.08	-32%
	Degree-of-Hybridisation for Block Energy (-)	0.0	0.0			
Typical PAX/Payload Off-Design Stage Length	Stage Length (nmi or km) and [PAX]	1111 [38]		600 [38]		
	Payload (kg or lbm)	3,686	3,686	8,127	8,127	-
	Block Fuel (kg or lbm)	1,538	1,950	3,443	4,300	-20%
	CO_2-Emissions (kg or lbm)	6,632	7,372	14,663	16,253	-9.8%
	Block Fuel per PAX (kg/PAX or lbm/PAX)	41.1	51.3	90.6	113	-20%
	CO_2-Emissions per PAX (kg/PAX or lbm/PAX)	174.5	194.0	385.9	427.7	-9.8%
	Block Energy (MWh or MBTU)	20.3	22.5	69.2	76.4	-9.5%
	Block Energy per PAX (MWh/PAX or MBTU/PAX)	0.53	0.59	1.82	2.01	
	Mission Energy Index (Wh/kg.km or BTU/lbm.nm)	4.96	5.48	14.18	15.68	-9.5%
	Degree-of-Hybridization for Block Energy (-)	17% climb / 23.5% cruise	0%			

Acknowledgments

This research was sponsored under NASA contract #NNX17AJ92A. The authors wish to thank Ray Beach at NASA in addition to the other ULI University PIs including Thomas Jahns at University of Wisconsin-Madison, Patrick McCluskey at University of Maryland, John Kizito at North Carolina A&T, and Jin Wang at OSU. The authors would also like to acknowledge Matilde D'Arpino, Prashanth Ramesh, and Yann Guezennec at OSU for contributing to the technical progress of this work.

References

[1] C. Perullo, A. Alahmad, J. Wen, M. D'Arpino, M. Canova, D. Mavris and M. Benzakein, "Sizing and Performance Analysis of a Turbo-Hybrid-Electric Regional Jet for the NASA ULI Program," in *AIAA Propulsion and Energy*, Indianapolis, IN, 2019.

[2] J. Gladin, C. Perullo, J. Tai and D. Mavris, "A Parametric Study of Hybrid Electric Gas Turbine Propulsion as a Function of Aircraft Size Class and Technology Level," in *55th AIAA Aerospace Sciences Meeting*, Grapevine, Texas, 2017.

[3] C. Perullo, J. Tai and D. Mavris, "A New Sizing and Synthesis Environment for the Design and Assessment of Advanced Hybrid Electric Aircraft Propulsion Systems," in *ISABE-2015-20286*.

[4] M. Shi, I. Chakraborty, J. C. Tai and D. N. Mavris, "Integrated Gas Turbine and Environmental Control System Pack Sizing and Analysis," in *2018 AIAA Aerospace Sciences Meeting*, Orlando, 2018.

[5] W. M. Kays and A. L. London, Compact Heat Exchangers, Third Edition, McGraw-Hill, 1984.

[6] M. Shi, M. Sanders, A. Alahmad, C. Perullo, G. Cinar and D. Mavris N, "Design and Analysis of the Thermal Management System of a Hybrid Turboelectric Regional Jet for the NASA ULI Program," in *To be published in AIAA Propulsion and Energy Forum 2020*, New Orleans, 2020.

[7] "Air Carrier Statistics Database (T-100)," DOE Bureau of Transportation Statistics, 2013. [Online].